IOSR Journal of Computer Engineering (IOSR-JCE)
e-ISSN: 2278-0661,p-ISSN: 2278-8727, Volume 20, Issue 2, Ver. II (Mar. - Apr. 2018), PP 16-26
www.iosrjournals.org

Analysis of a downdraft gasifier for energy use of biomass waste applying computational fluid dynamics

Randall Salazar Esquivel[1], Pedro Casanova Treto[1,2], Kattia Solís Ramírez[2]
[1](*Instituto de Investigaciones en Ingeniería (INII), Universidad de Costa Rica, Costa Rica)*
[2](*Escuela de Ingeniería de Biosistemas, Universidad de Costa Rica, Costa Rica)*
Corresponding Author: Randall Salazar Esquivel

Abstract: *A numerical modeling was performed that simulates the thermal and fluid-dynamic behavior and generation of chemical species from the biomass gasification process in a downdraft reactor using computational fluid dynamics (CFD). The simulation process was assumed as a stationary state, energy models, turbulence, transport of species and multiphase were established to adequately represent the equations that govern the transfer of mass, momentum and energy in the thermo-chemical degradation process of biomass. Variations in the airflow rate entered into the reactor were established in order to determine the optimum point of operation of the reactor. It was determined that using a flow rate of 400 l/min of air, the best results in terms of the quality of syngas produced are obtained, establishing this condition as the optimum operating point of the reactor.*

Keywords: *Biomass, CFD, downdraft gasifier, syngas.*

Date of Submission: 11-03-2018 Date of acceptance: 26-03-2018

I. Introduction

The study and characterization of various biomass as an energy resource has been a topic of investigation, which has been given greater attention in recent years, mainly because of its energy potential and global production volumes. The biomass gasification is a promising and efficient technology in energy production, which can contribute significantly to the generation of renewable energy [1].

Costa Rica has a great potential for the use of biomass waste for energy production. The production of ligno-cellulosic biomass waste, which can be used for the main agricultural activities at a national level (including pineapple, coffee, bananas, palm and rice, in order of highest to lowest production) reached 6,500,000.00 tons/year for 2010 approximately; this emphasizes the importance of implementing useful technologies in the energy use of this type of biomass [2].

The numerical methods applied in computational fluid dynamics can be used to describe these degradation processes of biomass in simpler components. These have become an important analysis and design tool to describe the flow and temperature patterns, the concentration of products and the gasification yields [3].

Modeling techniques in computational fluid dynamics (CFD) have become a useful tool in the area of thermochemical biomass conversion. Several researchers have used modeling in CFD to analyze the behavior of thermochemical conversion equipment; this has established itself as an effective complement for the development of new ideas and technologies, saving on costs, time and safety [4].

This investigation seeks to evaluate gasification as an alternative to the use of biomass waste, studying by modeling computational fluid dynamics behavior of the production of syngas to varied various physicochemical conditions which allow validating the implementation of this type of technology as an efficient tool for converting biomass into a renewable fuel.

II. Materials And Methods

The gasifier used for the investigation is a downdraft reactor shown in Fig. 1, designed and built by the Forest Resources Unit of the Institute of Engineering Research (INII) of the Universidadde Costa Rica. The main dimensions of the reactor are presented in Figure 2.

Fig 1. Concurrent flow gasification reactor.

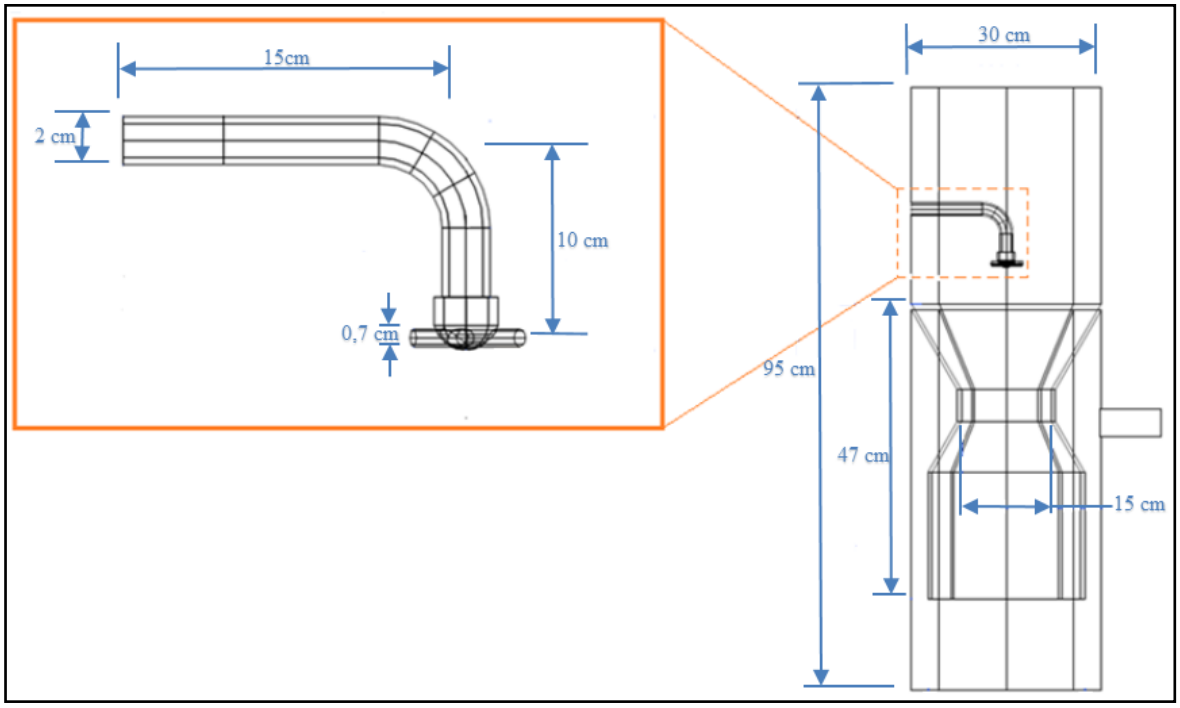

Fig 2. Characteristic dimensions of the concurrent flow gasifier.

2.1. Mathematical modeling

2.1.1. Mass balance model

The continuity equations for the gas and solid phase are given by [5]:

$$\frac{\partial}{\partial t}(\alpha_g \rho_g) + \nabla(\alpha_g \rho_g v_g) = S_{gs} \quad (1)$$

$$\frac{\partial}{\partial t}(\alpha_s \rho_s) + \nabla(\alpha_s \rho_s v_s) = S_{sg} \quad (2)$$

where:

α: volumetric fraction (cm^3)
ρ: density (g/cm^3)
υ: instantaneous velocity of the gas/solid phase (m/s)
S: mass source due to heterogeneous reactions (g), is expressed as [5]:

$$S_{sg} = -S_{gs} = M_C \sum \gamma_C R_C \quad (3)$$

where:

MC: molecular weight
γ C: stoichiometric coefficient
RC: reaction rate

The momentum equation of the gas phase is given by [5]:

$$\frac{\partial}{\partial t}(\alpha_g \rho_g v_g) + \nabla(\alpha_g \rho_g v_g v_g) = -\alpha_g \nabla p_g + \alpha_g \rho_g g + \beta(v_g - v_s) + \nabla \alpha_g \tau_g + S_{gs} U_s \quad (4)$$

where:

U_S: average speed of the solid (m/s)
β : drag coefficient of the gas-solid interface
τ_g: gaseous phase tensor stress (N)

2.1.2. Momentum model

The momentum equation of the solid phase is expressed as [5]:

$$\frac{\partial}{\partial t}(\alpha_s \rho_s v_s) + \nabla(\alpha_s \rho_s v_s v_s) = -\alpha_s \nabla p_s + \alpha_s \rho_s g + \beta(v_g - v_s) + \nabla \alpha_s \tau_s + S_{sg} U_s \quad (5)$$

where:

p_s: pressure of the particles due to collisions (Pa)
τ_s: tensile stress of the particle (N)

2.1.3. Turbulence model

Launder and Spalding [6] developed the standard κ-ε model derived from the average Reynolds equations of Navier-Stokes. By means of dimensional analysis, the turbulent viscosity μtcan be assumed as [7]:

$$\mu_t = C_\rho VL \quad (6)$$

where:

C: dimensionless constant
V: turbulent speed (m/s)
L: turbulent length (m)

According to the dimensional analysis, the turbulent speed scale (V) and the length scale (L) can be defined as [8]:

$$V = \kappa^{\frac{1}{2}} \text{and} L = \frac{\kappa^{\frac{2}{3}}}{\varepsilon} \quad (7)$$

where:

κ : turbulent kinetic energy (m^2/s^2)
ε : turbulent kinetic energy dissipation rate (m^2/s^3)

2.1.4. Granular Eulerian model

The kinetic theory of granular fluxes is commonly used in the Eulerian-Eulerian approach to obtain constitutive relationships for the solid phase [9].

The Eulerian-Eulerian approach has several advantages over the Eulerian-Lagrangian approach, the main one being the consumption of computational resources, which is less in the Eulerian-Eulerian approach, additionally, meshing, memory consumption and computational requirements are optimized using this focus on a numerical modeling [10].

The conservation equation for granular temperature, obtained from the kinetic theory of gases, is given by [9]:

$$\frac{3}{2}\left[\left(\frac{\partial(\rho_s\alpha_s\theta_s)}{\partial(t)}+\nabla(\rho_s\alpha_s\overrightarrow{v_s}\theta_s)\right)\right]=(-p_s\bar{I}+\overline{\tau_s}):\nabla(\overrightarrow{v_s})+\nabla\left(k_{\theta_a}\nabla(\theta_s)\right)-\gamma_{\theta_a}+\emptyset_{ls}(8)$$

where:

$(-p_s\bar{I}+\overline{\tau_s}):\nabla(\overrightarrow{v_s})$: power generation by the efforts in the solid
$k_{\theta_a}\nabla(\theta_s)$: diffusion energy
k_{θ_a}: diffusion coefficient
γ_{θ_a}: energy collision dissipation
$\emptyset_{ls}$: energy exchange between the gas phase and the solid phase

2.1.5. Chemical reactions model

The transport of species is a useful tool for predicting reaction times or chemical reactions. For species i', the conservation equation for the mass fraction of that species is given as follows [11]:

$$\frac{\partial}{\partial t}(\rho m_{i'})+\frac{\partial p}{\partial X_i}(\rho U_i m_i)=\frac{\partial}{\partial X_i}J_{j',i}+R_{i'}+S_{i'}(9)$$

where:

$J_{j',i}$: componenti of the diffusion flow of species j' in the mixture
$R_{i'}$:velocity at which species are consumed or occur in one or more reactions [7]

This model considers a relationship between the reaction rate, the rate of dissipation of reactants and products containing eddies, suggesting that the reaction rate may be the lesser of the following two expressions [12]:

$$R_{i',\kappa}=v_{i',k}M_{i'}A\rho\frac{\varepsilon}{\kappa}\frac{m_R}{V_{R',k}M_p}(10)$$

$$R_{i',\kappa}=v_{i',k}M_{i'}AB\rho\frac{\varepsilon}{\kappa}\frac{m_p}{V_{R',k}M_p}(11)$$

where:

m_p: mass fraction of the produced P species
m_R: mass fraction of reactant R species
A, B: empirical constants equal to 4.0 and 0.5
ϵ/κ: time scale of turbulent eddies

1.1.6. Conservation of energy

To describe the conservation of energy, the following conservation equation must be solved for each phase [5]:

$$\frac{\partial(\alpha_q\rho_q h_q)}{\partial(t)}+\nabla\left(\alpha_q\rho_q\overrightarrow{u_q}h_q\right)=-\alpha_q\frac{\partial(p_q)}{\partial(t)}+\overline{\tau_q}:\nabla(\overrightarrow{u_q})-\nabla\overrightarrow{q_q}+S_q+\sum_{p=1}^{n}\left(\overrightarrow{Q_{pq}}+\dot{m}h_{pq}-\dot{m}h_{qp}\right)(12)$$

where:

h_q: specific enthalpy of phase qth (kJ/kg)
$\overrightarrow{q_q}$: heat flux (W/m^2)
S_q: term product of chemical reactions
Q_{pq}: heat transfer between phases pth and qth (W)
h_{pq}: enthalpy of the interface (kJ/kg)

1.2. Modeling environment

The geometric model was designed using Inventor® software and imported into ANSYS Workbench 18.0, the mesh was made and subsequently exported to FLUENT, where physical models, boundary conditions and material properties were established.

2.2.1. Preparation of the CAD model

Figure 3 shows the detail of the geometric model with which the numerical modeling of the concurrent flow gasifier was developed.

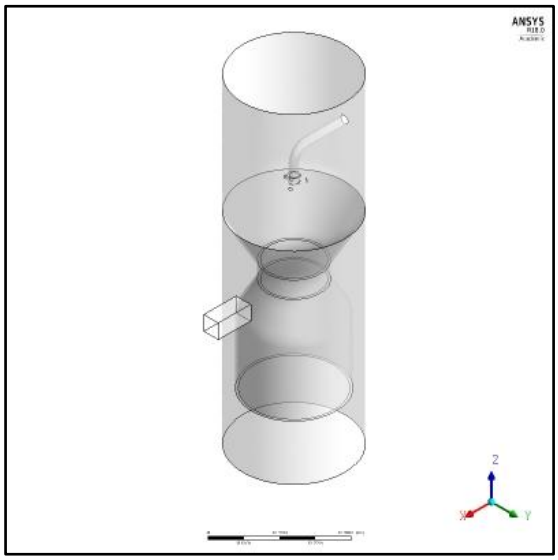

Fig 3. Geometric model used in computational fluid modeling.

2.2.2. Discretization of the domain

Meshing is a key part of the quality and convergence of the solutions. The discretization of the domain was based on the finite volume method, by means of the decomposition of the domain into small control volumes, generating a three-dimensional mesh of nodes. The finite volume method considers the principles of conservation of mass, momentum and energy, which are the basis of fluid-dynamic mathematical modeling.

For the present case, a mixed mesh between tetrahedral and hexahedral elements was used, generating a mesh with a total number of nodes of 39160 and 210792 elements, presenting an orthogonal quality of 0.859 ± 0.085 and an obliquity value of 0.227 ± 0.122.

2.3. Properties and characterization of materials

The modeling of the interior of the gasifier consists of two phases, a first phase of volatile compounds that make up the synthesis gas, the second phase consists of sawdust pellets and air, corresponding to the solid phase. As part of the mix of sawdust pellets and air corresponding to the granular phase, it was necessary to establish physical parameters that would identify the sawdust pellets as the raw material to carry out the set of chemical reactions that give way to gas generation of synthesis.

For the characterization of this material, we took as reference the data generated by Carrillo [13], in his study of physical-chemical properties of pellets made from sawmill waste. Table 1 presents physical and thermal properties that were used to characterize the material during numerical modeling.

Table 1. Physical and thermal properties of pellets made from sawmill waste [13].

Characterization of sawdust pellets	
Unit density (kg/m^3)	1105.04
Bulk density (kg/m^3)	552.3
Specific heat (kJ/kg·K)	2.183
Thermal conductivity (W/m·K)	0.279
Porosity (%)	50.02

2.4. Boundary conditions

The boundary conditions are responsible for specifying the flow, chemical and thermal variables at the limits of the physical model.

Three different mass airflowswere used in the modeling performed; the amount of air to enter the reactor was based on the experimental studies carried out by Guangul et al [14] in a concurrent flow gasifier, conditions similar to those being treated in the present study.

A flow rate of 400 l/min was established as the base flow so that the necessary conditions for the gasification process are presented, Guangul et al [14] indicate that by entering this amount of air into the reactor stable conditions were maintained for the production of syngas . In a complementary way, we worked with flow rates of 300 l/min and 500 l/min, Guangul et al [14] concluded these flows as the limit ranges for the thermochemical processes in the gasification reactor to be carried out.

Considering the flow rates of the gasifying agent that were compared during the CFD study, three different case studies are obtained; In order to simplify the understanding of the results, the notation described in Table 2 will be used.

Table 2. Case studies proposed for the numerical modeling of the gasification reactor.

Case	Flow (l/min)
I	300
II	400
III	500

2.5. Validation of the numerical model

Due to the stage in which the INII research project is located, experimental data on temperature, velocities and synthesis gas composition that validate the consolidated numerical model are not available.Therefore, the validation of the model was carried out by comparing the mass fractions of the species that make up the synthesis gas obtained with respect to the syngas composition reported in various investigations of concurrent bed gasification reactors [15, 16, 17, 18, 19, 20, 21]. The reliability of the numerical model generated was examined using the root mean square error, recommended to study the accuracy in computational fluid dynamics models [22], the equation of said error are shown in equation 13. Errors less than 10%are considered acceptable in the case of numerical models that simulate combustion and / or gasification conditions [23].

$$RMSE = \sqrt{\frac{1}{n}\sum_{i=1}^{n}(y_{mod,i} - \bar{y}_{dato})^2} \quad (13)$$

where:

n: amount of data

$\bar{y}_{dato}$: average of the data measured in different investigations carried out

$y_{mod,i}$: value obtained from the simulation

III. Results

3.1. Dynamic and thermal behavior of the gasifier

Figure 4 shows the spatial distribution of the flow of volatile species for case II. From this case, the rapid dissipation of the airflow velocity entered into the reactor is observed, product of the porous pellet bed that is inside the reactor. The collision of the flow of air directly with the walls of the reactor causes recirculation of the flow in this area, generating the increase of turbulence in the upper zone of the gasifier, turbulence represented graphically by the generation of eddies in the upper strata of the reactor.

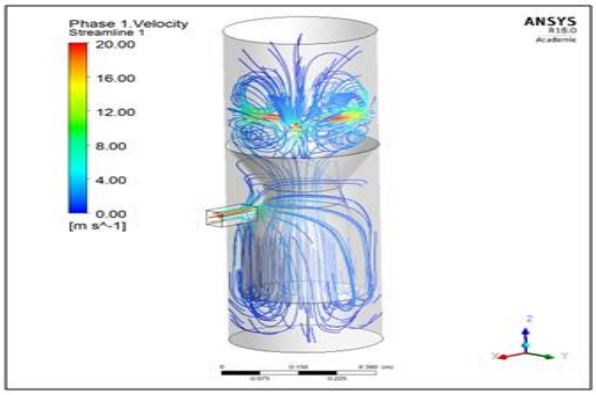

Fig 4. Speed distribution and flow line patterns of the volatile phase for case II.

The effect of turbulence and a greater interaction of the air in the upper zone of the reactor causes a greater reaction between the gas phase and the solid bed of pellets. It implying a direct increase of the temperature in this zone, where a maximum temperature of 1050 ° C, this effect is illustrated in Figure 5, where the temperature distribution in the porous bed is shown. The reason that this high temperature point is reached is mainly due to the amount of oxygen present in this area of the reactor and the reaction of the CO, exothermic reaction whose release of energy results in the increase of the temperature in the gasifier.

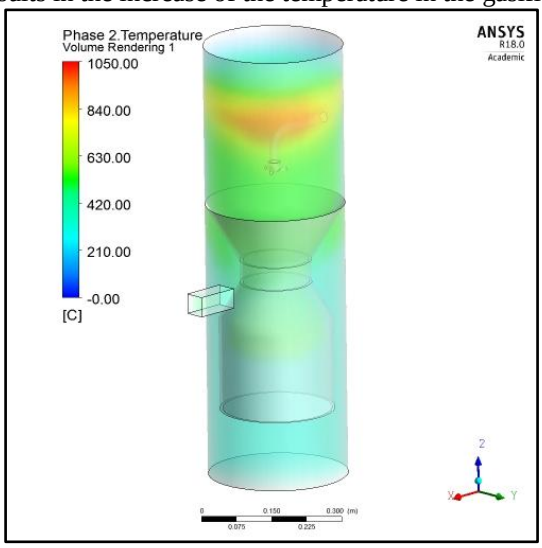

Fig 5. Temperature distribution in the gasifier for case II.

When this high temperature focus appears in the upper area of the reactor, the combustion or oxidation zone is displaced, a situation that directly affects the release and consumption of chemical species, hence the efficiency of the gasifier.

Sheth&Babu [24], when conducting experimental studies of syngas production from wood waste in a concurrent flow gasifier, determined that the average temperature of the reactor in the area where the air is enteredis 1000 °C, and the average temperature of the pyrolysis zone around 500 °C. Sharma [6] in modeling the transport dynamics in the porous medium of a concurrent bed gasifier, established that the temperature ranges in the reactor body varied from 950 °C to 200 °C.

Figure 6 and Figure 7 show the dynamics of the volatile flow lines and the temperature distribution in the gasifier respectively, this for case I.

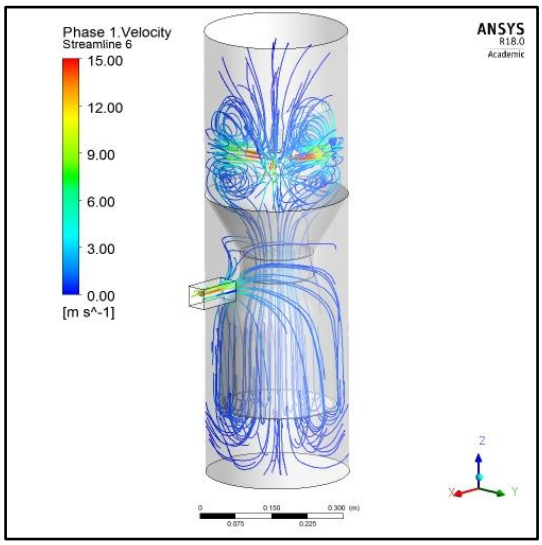

Fig 6. Speed distribution and flow line patterns of the volatile phase for case I.

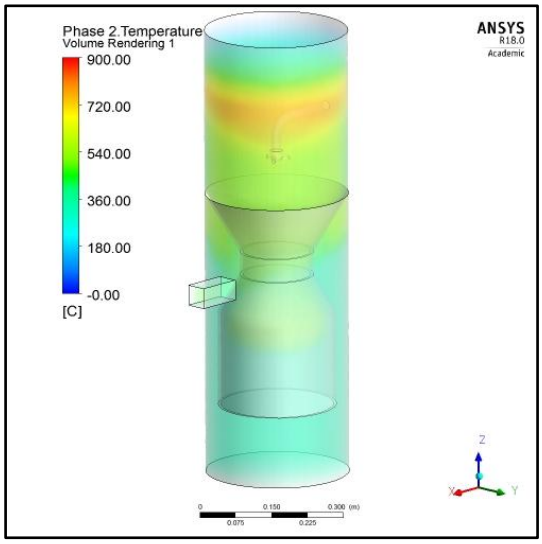

Fig 7. Temperature distribution in the gasifier for case I.

Figure 6 shows a decrease in speed when reducing the flow rate entered into the reactor. The pattern of recirculation of air in the upper zone of the reactor presents a behavior analogous to that of case II. This behavior causes the high temperature zones in these upper strata, as indicated in Figureure 8, however, there is a marked decrease in temperature throughout the reactor bed, an aspect caused by the reduction of oxygen input, limiting the processes combustion and release of volatile gases specific to gasification.

Figure8 and 9 show the dynamics of the volatile flow lines and the temperature distribution in the gasifier, respectively, when the airflow rate entered into the reactor is 500 l/min. There is a marked increase in the gas flow velocity for this condition, maintaining, as is the case in the previous scenarios, high turbulence patterns in the upper part of the gasifier.

For the presented conditions the increase of the temperatures in all the strata of the reactor is observed, aspect caused by the increase of the entered oxygen. This is counterproductive for chemical reactions, since the optimum stoichiometry ratio is affected so that the gasification process is carried out, promoting the process to become a complete combustion, where inert gases with low energy content such as CO and CO_2 are produced in greater quantity, affecting the energy efficiency of the generated syngas.

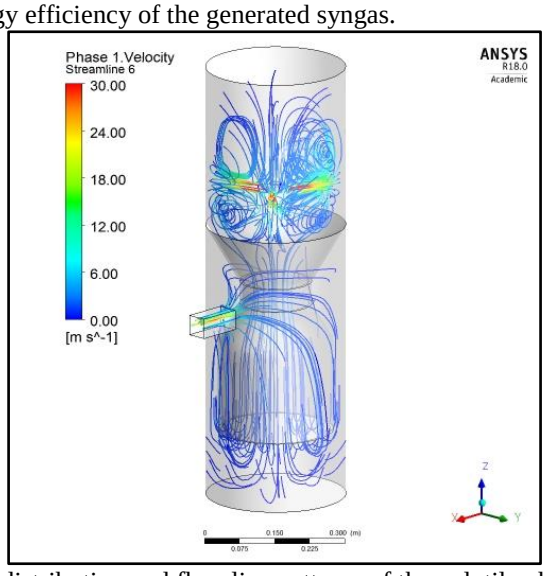

Fig 8. Velocity distribution and flow line patterns of the volatile phase for case III.

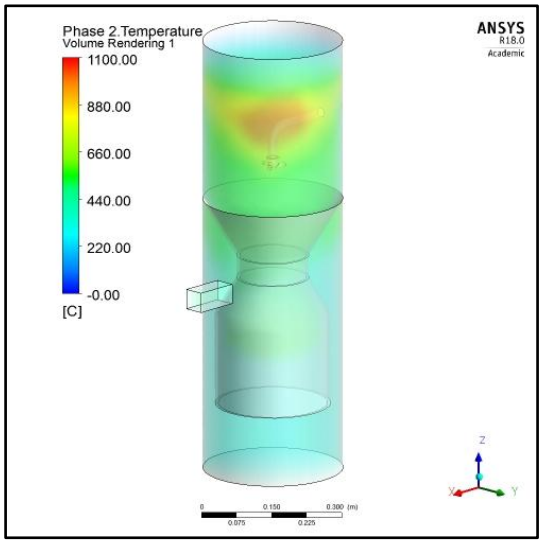

Fig 9. Temperature distribution in the gasifier for case III.

The behavior shown by the temperature parameter in the nine modeled scenarios presents several variations to the theoretical behavior that is expected from a concurrent bed gasifier. There is also no clear transition in temperature changes. It indicate the stage of gasification that is taking place in a certain reactor position, an effect of the recirculation movement of the airflow in the gasifier. Although these characteristic temperature strata do not occur in these reactors, the temperature ranges obtained are similar to those that the theory indicates.

The effect of the liberation, consumption and final formation of the chemical species that participate in the gasification process is analyzed; their composition varies due to the temperatures, quantity of oxygen and chemical reactions (exothermic and endothermic) that occur in the different stages of the process.

CO and CO_2 are chemical compounds that do not represent any significant energy potential in the composition of syngas. The generation of these species to the minimum extent possible is beneficial for the increase in the quality of synthesis gas, since, it promotes the release of species that do have a high energy value in syngas, such as CH_4 and H_2. The proportions of CO and CO_2 increase when the gasification conditions are not adequate, that is, excess or lack of oxygen in the thermochemical process.

The effect of varying the flow of air entering the gasifier in the formation of chemical species present in the synthesis gas is shown in Figure 10. When a flow rate of 400 l/min is used, a marked decrease in the concentration of CO and $CO_2$is observed. Increasing or decreasing this flow translates into a significant increase in the mass fraction of these chemical species.

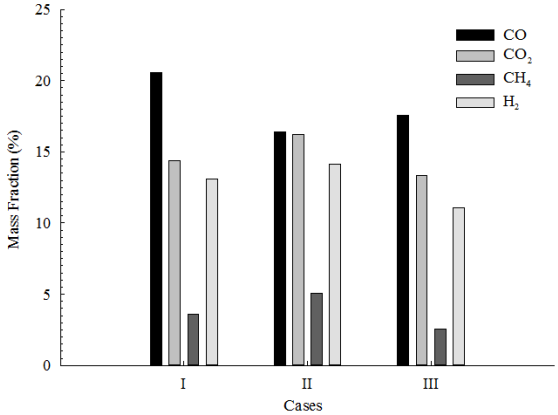

Fig 10. Variation of chemical species present in the syngas according to each case analyzed.

As for the methane concentration, when using the flow rate of 400 l/min, the largest mass fractions of the modeling are obtained, this indicates that using this flow will result in a higher quality energy synthesis gas.

By varying the flow rate of 400 l/min, there is a drastic reduction in the concentration of this chemical species, directly affecting the quality of the syngas.

The production of hydrogen contained in the syngas presents a behavior similar to that shown by methane in the previous case. The highest levels of hydrogen obtained are achieved by using a flow rate of 400

l/min, lower and higher flow rates at this flow cause a marked decrease in the concentration of hydrogen, therefore, energetically, the syngas produced from the flow of 400 l/min is of higher quality. This amount of air entered reduces the formation of CO and CO_2, increasing the CH_4 and H_2 formation, desirable conditions for a syngas of optimum quality.

3.3. Validation of the numerical model established for the gasification process

The composition of the synthesis gas obtained in the different numerical modeling performed with respect to the syngas composition reported in different scientific investigations is compared statistically; the results obtained for the three different cases presented in the investigation are shown in table 3.

Table 3. Mass fractions obtained in the conformation of the syngas for each case presented in the numerical modeling.

Flow (l/min)	CO (%)	CO_2 (%)	CH_4 (%)	H_2 (%)
300	20.55	14.36	3.58	13.08
400	16.39	16.22	5.05	14.12
500	17.54	13.36	2.57	11.08

Table 3 allows a better quantification of the results shown in Fig. 10, where the lower levelsof CO and $CO_2$are obtained for the flow of 400 l/min. The highest levels of CH_4 and H_2 are also present; the other two flows have deficiencies in the formation of these chemical species in order to obtain a synthesis gas of adequate composition.

Table 4 shows the mean square errors reported for each chemical species in each case study.

Table 4. Statistical validation of the results obtained in the conformation of the syngas reported in each numerical model.

Flow (l/min)	RMSE CO (%)	RMSE CO_2 (%)	RMSE CH_4 (%)	RMSE H_2 (%)
300	5.89	3.16	1.74	2.53
400	3.44	2.99	2.67	2.95
500	3.83	3.66	1.65	2.84

Table 4 denotes the validation of the results obtained for each chemical species that makes up the synthesis gas in each simulated configuration. The mean square errors for each species reported do not exceed 10% error, this implies that the results determined by the numerical model established are reliably linked to the results reported by various authors, so it can be considered that the established model represents with acceptable precision the chemical composition of the synthesis gas produced.

IV. Conclusion

There is a greater accumulation of turbulence in the upper strata of the gasification reactor for all the simulated scenarios, implying a direct increase in temperature in this area, directly affecting the release and consumption of chemical species in the reactor.

The flow of gasifying agent entering the gasification reactor has a direct effect on the temperature distribution in the different strata of the reactor, generating a direct effect on the chemical reactions that take place in the process.

The mass fractions of CO and CO_2 presented their lowest values when using a flow rate of 400 l/min. The highest levels of methane and hydrogen production are achievedby using a flow rate of 400 l/min.

Acknowledgements

The authors gratefully acknowledge the financial support of Central American Network of Engineering Institutions (REDICA), British Embassy, Universidad de Costa Rica (UCR), and Research and Development Network in Energy Efficiency and Renewable Energy (RIDER) of Universidad de Costa Rica.

References

[1]. Intelligent Energy Europe. Final guideline for safe and eco-friendly biomass gasification. Bruselas: EuropeanCommission; 2009. 10 p.
[2]. Roldán VC. Informe de capacidad de energías limpias en Costa Rica 2010. Cartago, Tecnológico de Costa Rica, Escuela de Química, 2010.
[3]. Herguido J, Corella J, González-Saiz J. Steam gasification of lignocellulosic residues in a fluidized bed at a small pilot scale. Effect of the type of feedstock. IndEngChem Res. 1992;31(5):1274–82.
[4]. Wang Y, Yan L. CFD Studies on Biomass Thermochemical Conversion. Int J Mol Sci. 2008;9:1108-30.

[5]. Magnussen BF, Hjertager BH. On mathematical Modeling of turbulent combustion with special emphasis on soot formation and combustion. En: 16th symposium (international) on combustion. Pittsburgh, EstadosUnidos; 1976 Agosto 15-20. p. 719–29.
[6]. Sharma AK. Modeling fluid and heat transport in the reactive, porous bed of downdraft (biomass) gasifier. Int J Heat Fluid Flow. 2007;28(6):1518–30.
[7]. Babu BV, Chaurasia AS. Pyrolysis of biomass: improved models for simultaneous kinetics and transport of heat, mass and momentum. Energy Convers Manag. 2004;45(9-10):1297–327.
[8]. Willcox DC. Turbulence modeling for CFD. 3rd ed. California: DCW Industries; 1998.
[9]. ANSYS ®. ANSYS FLUENT theory guide [Internet]. Canonsburg; 2013. Disponibledesde: https://uiuc-cse.github.io/me498cm
[10]. fa15/lessons/fluent/refs/ANSYS Fluent Theory Guide.pdf
[11]. Chapman S, Cowling TG. The mathematical theory of non-uniform gases. 3rd ed. Cambridge: Cambridge University Press; 1970.
[12]. Schlichting H, Gersten K. Boundary layer theory. 9th ed. Berlin: Springer; 2017.
[13]. Balcha DA. Numerical modeling of small-scale biomass straw gasifier [tesis de maestría]. Winnipeg: University of Manitoba; 2009.
[14]. Carrillo TP. Caracterización de pellets con fines energéticos elaborados a partir de residuos forestales [tesis de licenciatura]. San José: Universidad de Costa Rica; 2015.
[15]. Guangul FM, Sulaiman SA, Ramli A. Study of the effects of operating factors on the resulting producer gas of oil palm fronds gasification with a single throat downdraft gasifier. Renew Energy. 2014;72:271–83.
[16]. Babu BV, Sheth PN. Modeling and simulation of reduction zone of downdraft biomass gasifier: Effect of char reactivity factor. Energy Convers Manag. 2005;47(15-16):2602–11.
[17]. Couto ND. Energetic and exergetic analysis of biomass gasification [tesis de maestría]. Vila Real: University of Trás-os-Montes e Alto Douro; 2015.
[18]. Couto N, Silva V, Monteiro E, Brito P, Rouboa A. Using an Eulerian-granular 2-D multiphase CFD model to simulate oxygen air enriched gasification of agroindustrial residues. Renew Energy. 2015;77:174–81.
[19]. Gagliano A, Nocera F, Patania F, Bruno M, Castaldo D. A robust numerical model for characterizing the syngas composition in a downdraft gasification process. ComptesRendusChim. 2016;1–9.
[20]. Meenaroch P, Kerdsuwan S, Laohalidanond K. Development of kinetics models in each zone of a 10 kg/hr downdraft gasifier using computational fluid dynamics. Energy Procedia. 2015;79:278–83.
[21]. Silva V, Monteiro E, Brito P, Rouboa A. Experimental and numerical analysis of biomass gasification. Energy Procedia. 2013;36:591–5.
[22]. Gerun L, Bellettre J, Tazerout M. Investigation of the oxidation zone in a biomass two-stage downdraft gasifier. En: 18th International Conference on Efficiency, Cost, Optimization, Simulation and Envieronmental Impact of Energy Systems (ECOS 2005). Trondheim, Noruega; 2005 Junio 20-22.
[23]. Kobayashi K, Salam MU. Comparing simulated and measured values using mean squared deviation and its components. Agron J. 2000;92:345–52.
[24]. Darki EE. Modeling and economic assessment of integrated gasification with sorbent CO2 capture [tesis de doctorado]. Calgary: University of Carlgary; 2014.
[25]. Sheth PN, Babu B V. Experimental studies on producer gas generation from wood waste in a downdraft biomass gasifier. Bioresour
[26]. Technol. 2009;100(12):3127–33.

IOSR Journal of Computer Engineering (IOSR-JCE) is UGC approved Journal with Sl. No. 5019, Journal no. 49102.

Randall Salazar Esquivel "Analysis of a downdraft gasifier for energy use of biomass waste applying computational fluid dynamics" IOSR Journal of Computer Engineering (IOSR-JCE) 20.2 (2018): 16-26.